



HAL
open science

Effect of stress on water retention of needlepunched geosynthetic clay liners

Hajer Bannour, Guillaume Stoltz, Pierre Delage, Nathalie Touze

► **To cite this version:**

Hajer Bannour, Guillaume Stoltz, Pierre Delage, Nathalie Touze. Effect of stress on water retention of needlepunched geosynthetic clay liners. *Geotextiles and Geomembranes*, 2014, 42 (6), pp.629-640. 10.1016/j.geotexmem.2014.09.001 . hal-01774672

HAL Id: hal-01774672

<https://enpc.hal.science/hal-01774672>

Submitted on 15 May 2018

HAL is a multi-disciplinary open access archive for the deposit and dissemination of scientific research documents, whether they are published or not. The documents may come from teaching and research institutions in France or abroad, or from public or private research centers.

L'archive ouverte pluridisciplinaire **HAL**, est destinée au dépôt et à la diffusion de documents scientifiques de niveau recherche, publiés ou non, émanant des établissements d'enseignement et de recherche français ou étrangers, des laboratoires publics ou privés.

1 **EFFECT OF STRESS ON WATER RETENTION OF**
2 **NEEDLEPUNCHED GEOSYNTHETIC CLAY LINERS**

3
4 Bannour. H.⁽¹⁾. Stoltz. G.⁽²⁾. Delage. P.⁽³⁾ and Touze Foltz. N.^{(4)*}

5 ⁽¹⁾ Irstea. HBAN Unit. Antony. France. Tel: +33-1 40 96 65 25; Fax: +33-1 40 96 65 25; E-mail: hajer.bannour@irstea.fr

6 ⁽²⁾ Irstea. HBAN Unit. Antony. France. Tel: +33-1 40 96 60 39; Fax: +33-1 40 96 60 48; E-mail: guillaume.stolz@irstea.fr

7 ⁽³⁾ Ecole des Ponts ParisTech, Navier/CERMES , France. Tel: +33-1 64 15 35 42; Fax: + 33-1 64 15 35 42; Email : delage@cermes.enpc.fr

8 ^{(4)*} Corresponding author: Irstea. HBAN Unit. Antony. France. Tel: +33-1 40 96 60 39; Fax: +33-1 40 96 62 70; E-mail:
9 nathalie.touze@irstea.fr

10
11 **ABSTRACT**

12 Geosynthetic clay liners (GCLs) are placed at the bottom of waste disposal facilities where they hydrate
13 from the subsoil and eventually from a hydraulic head on geomembranes (GMs) defects. Predicting hydration
14 behavior of GCLs requires knowledge of the water-retention properties of the GCL along wetting paths. Given
15 that GCLs could be subjected to different ranges of vertical stresses that are induced by the weight of the
16 supported waste, the confining stress could affect water-retention properties of GCLs and should be investigated.
17 To do so, a laboratory methodology to establish the water-retention curves (WRCs) of needlepunched GCLs
18 under stress was undertaken. Various constant vertical stresses corresponding to different weights of the
19 supported waste were applied to GCL specimens placed in controlled-suction oedometers. Suction values were
20 selected so as to mimic a wetting path from the initial dry state to zero suction. Suction was controlled by using
21 controlled suction techniques with controlled humidity imposed by a saturated saline solutions and using the
22 osmotic technique with polyethylene glycol (PEG) solutions. Measurements were undertaken on oedometer
23 systems as to apply confining stresses and have been complemented by standard saturated oedometer swelling
24 tests. The data obtained confirm that increasing the stress on to the GCL results in less, albeit faster, water
25 uptake, which could emphasize on recommendations about rapidly covering GCLs after they are placed at the
26 bottom of a waste disposal facilities. Finally, the potential validity of the state-surface concept, which was
27 developed in unsaturated soil mechanics, is discussed using van Guenuchten's and Fredlund and Xing's
28 equations for water retention curves.

29 *Keywords: geosynthetics, geosynthetic clay liner, unsaturated conditions, water retention curve, suction,*
30 *confining stress.*

31

1. INTRODUCTION

Geosynthetic clay liners (GCLs) are composite materials used in geotechnical and geoenvironmental engineering applications. Specifically, they serve as barrier systems in landfill liners, tailing ponds or dams (Bouazza, 2002). GCLs have gained worldwide acceptance because once they are hydrated and confined, they represent excellent hydraulic barriers. GCLs consist of a layer of bentonite inserted between two geotextiles linked together by various means (stitching, needle punching, heat bonding, wrapping, etc.). The suction of the bentonite contained in GCLs can be as high as 1000 MPa (Beddoe et al., 2010).

When installed in composite liners, GCLs hydrate under a compressive stress corresponding to the overburden load. After that, the GCL hydrates typically from both the liquid flux through defects in the geomembrane (GM) and the transfer of vapour and liquid water from the underlying soil through the GCL (Azad et al., 2011; Beddoe et al., 2010). Assuming a typical depth of waste deposits of between 20 and 30 m and adopting a density of 800 to 1000 kg/m³ for the waste, vertical stresses applied to GCLs at the bottom of deposits may reach 300 kPa.

The capability of a GCL to serve as a barrier to fluids (either liquid or gas) is intimately linked to the uptake of moisture by the bentonite. However, there is no guarantee that the GCL will reach full hydration before leakage begins through a defective geomembrane. Accurately predicting the hydraulic behavior of composite liners requires knowledge of both the water retention curve (WRC) of the GCL and its volumetric changes during hydration. Many experimental studies have investigated the water-retention properties of GCLs (Daniel et al., 1993; Barroso et al., 2006b; Southen and Rowe, 2007; Abuel Naga and Bouazza., 2010; Beddoe et al., 2010; Beddoe et al., 2011; Hanson et al., 2013; see Table 1). In addition, to quantifying the transient hydration of GCLs under experimental unsaturated conditions,

57 Siemens et al. (2011, 2013) have done numerical simulations on the transient hydration of
58 GCLs. They assessed the impact of two confining stresses (10, 100 kPa) on the rate of
59 hydration and the moisture equilibrium content of GCLs.

60 Most investigations into water retention in the wetting path (Daniel et al., 1993; Barroso et al.,
61 2006; Beddoe et al., 2010; 2011; Hanson et al., 2013) have been done without considering the
62 confining stress effect which affects the water-retention properties of the GCL (as observed in
63 other bentonite-based materials). For example, in radioactive waste management, Yahia-Aissa
64 et al. (2001) demonstrated that volume constraint of compacted bentonite leads to
65 significantly less water retention at saturation. This effect was later confirmed by Lloret et al.
66 (2003) and Villar et al. (2003), who used the same approach. Southen and Rowe (2007)
67 investigated the effect on water-retention in GCLs of different confining stresses (3 and 100
68 kPa) applied along a drying path. The effect of confining stress applied along a wetting path
69 was investigated by Abuel-Naga and Bouazza (2010) (with a single stress of 50 kPa) and by
70 Beddoe et al. (2011) (with a small stress of 2 kPa). Siemens et al. (2013) numerically studied
71 the effect of confining stresses of 2 kPa and 100 kPa on water retention in GCLs.

72 These studies did not investigate water retention along a wetting path for the larger range of
73 confining stresses that corresponds to deeper waste deposits (for example in the case when a
74 hydraulic head exist on the GM overlying the GCL is presenting holes).

75 To better understand the hydromechanical response of GCLs, this paper presents the results of
76 an experimental program designed to investigate the effect of confining stress applied along
77 the wetting path of the WRC of GCLs. The WRC was determined based controlled suction
78 techniques adapted to oedometer equipment with saturated saline solutions and osmotic
79 technique with polyethylene glycol (PEG) solutions. Measurements were complemented by
80 standard saturated oedometer swelling tests to obtain water retention properties at zero
81 suction. In the following, WRCs at the wetting path, their experimental determination, and

82 their relevance with respect to GCL issues are first briefly introduced. Second, the suction-
83 control methods that were applied to the GCL are described. Finally, the results obtained are
84 presented and compared with published data. Two well-known WRC equations (van
85 Guenuchten's and Fredlund and Xing's) are fit to the data obtained and an explanation of the
86 effect of stress is proposed.

87

88 **2. WATER-RETENTION CURVES**

89 **2.1. Water-retention along wetting path in geosynthetic clay liners**

90 GCLs have a composite structure consisting of geotextiles and bentonite. When the GCL is
91 under unsaturated conditions, Abuel Naga and Bouazza (2010) modeled the structure of a
92 GCL as a double-porosity material with two distinct air-entry values and two residual water
93 contents corresponding to that of the geotextile and that of the bentonite. Based on the fact
94 that GCLs present composite structures, along the wetting path, the GCL's bentonite will
95 swell and could squeeze out to occupy some of the pore space of the geotextile component
96 with the confining stress .

97 In this context, it is important to find a suitable methodology for investigating the water
98 retention of GCLs along the wetting path over the entire relevant suction range by examining
99 the effects of confining stress on GCL water retention.

100 **2.2. Techniques to determine water-retention curve of geosynthetic clay liner**

101 Some methods recently adopted to determine the WRCs of GCLs have been described by
102 Abuel Naga and Bouazza (2010), Beddoe et al. (2010), and Zornberg et al. (2010). Based on
103 Figure 1, it is recommended to combine at least two different techniques to cover the entire
104 suction range of GCLs. As seen in Table 1, methods used to determine the WRC of GCLs
105 include (i) vapour equilibrium (Daniel et al. 1993) and (ii) axis-translation techniques based
106 on plates or membrane extractors (Southen and Rowe, 2004; 2007; Hanson et al., 2013). (iii)

107 thermocouple psychrometer (Daniel et al., 1993; Abuel-Naga and Bouazza, 2010), (iv) the
108 filter-paper technique (Barroso et al., 2006b; Hanson et al., 2013), (v) high-capacity
109 tensiometers (Beddoe et al., 2010 ; 2011), and (vi) capacitive relative-humidity sensors
110 (Abuel Naga and Bouazza, 2010 ; Beddoe et al., 2010 ; 2011 ; Hanson et al., 2013).

111 Some methods have shown their limitations for use with GCLs. For example, sensors such as
112 thermocouple psychrometers are irrelevant at low suction (<1 MPa), particularly because of
113 their significant temperature sensitivity (Daniel et al., 1993; Abuel Naga and Bouazza, 2010),
114 and fungi that develop on filter paper could affect the results of the filter-paper technique if
115 test protocol is not followed (Barroso et al., 2006b).

116 This study used to present an original methodology for establishing water retention curve of
117 GCLs under wetting path and confining stress that takes into account the composite structure
118 of GCLs.

119

120 **3. MATERIALS AND METHODS**

121 **3.1. Geosynthetic clay liner properties and preparation**

122 A needle-punched GCL containing granular sodium bentonite was used. The cover
123 geotextile was woven and the carrier geotextile was needle punched. The mass per unit area
124 M_b of bentonite was 5.80 kg/m². The average thickness of the GCL was 7 mm. The basic
125 features of the measurements done to determine the WRCs of the GCL are summarized in
126 Table 2. The GCL sample was cut into 7-cm-diameter specimens by using a cookie cutter and
127 then inserted in the oedometer in which suction-control methods were applied under various
128 stresses. These methods are presented in Sections 3.2.1 and 3.2.2.

129 To obtain results that are independent of the GCL bulk void ratio, specimens were selected to
130 ensure a relatively uniform mass per unit area M_b of bentonite. The selection has been made
131 by cutting 20 GCL specimens then chooses the closest values of mass of GCLs.

132 **3.2. Techniques to establish the water retention curve of geosynthetic clay liner**

133 Three methods were used to determine water retention curve of geosynthetic clay liner. Two
134 method were used to control the suction using saturated saline solutions (controlling the total
135 suction), and the osmotic technique (controlling the matric suction). These two techniques
136 were adapted to oedometer cells where GCL specimens were confined. It is not necessary to
137 adjust total suction values for the matric suction controlled by the osmotic oedometers
138 because it was deemed irrelevant for the range of total suctions measured for GCLs (Beddoe
139 et al. 2011). This approach allowed (i) the application of a controlled vertical stress; and (ii)
140 the coverage of the wide range of suction required to establish the WRC of the GCL along the
141 wetting path starting from the natural water content. An additional standard saturated
142 oedometric measurement was also done to obtain data at zero suction.

143 **3.3. Method used to control geosynthetic clay liners' suction**

144 **3.3.1. Control of relative humidity of vapour by oversaturated salt solution (SS** 145 **measurements)**

146 This technique consists of controlling the total suction by controlling the relative humidity
147 around the specimen in a closed loop in which the vapour generated by oversaturated salt
148 solutions (SS) is circulated. This technique is preferably used with relative humidity less than
149 97% (suction greater than 4.2 MPa). The suction applied depends on the nature of the salt
150 used, on temperature, and on air pressure. In this study, the vapour-equilibrium technique was
151 used to hydrate the GCL starting from its initial situation.

152 The relative humidity R_H is linked to suction ψ through Kelvin's law:

$$153 \quad \psi = u_a - u_w = -\frac{RT}{Mg} \ln(R_H), \quad (1)$$

154 Where ψ is the suction (MPa), u_a is the air-pore pressure (MPa), u_w is the water-pore pressure
155 (MPa), R is the universal gas constant ($R = 8.314 \text{ J}\cdot\text{Mol}^{-1}\cdot\text{K}^{-1}$), T is the temperature in

156 kelvins, M is molecular weight of water (18×10^{-3} kg/mol), and g is the acceleration due to
157 gravity (m/s^2).

158 In this study, two different salts were used: potassium sulfate (K_2SO_4) and potassium nitrate
159 (KNO_3). Their chemical properties at 20°C are presented in Table 4. The suction applied is
160 4.2 MPa for K_2SO_4 and 8.5 MPa for KNO_3 .

161

162 3.3.2. Control of matric suction using osmotic technique

163 The osmotic technique (Delage and Cui 2008) is based on controlling the matric suction by
164 using a polyethylene glycol (PEG) solution at various concentrations. The concentrations are
165 determined by a calibration curve initially proposed by Williams and Shaykewich (1969). The
166 osmotic method makes it possible to control suction from 0 to 10 MPa (Delage et al. 1998).
167 The most common PEGs used in geotechnical measurements have a molecular weight of 6000
168 or 20000 Da ($1 \text{ Da} = 1.66^{-24} \text{ g}$) (Delage and Cui, 2008). The calibration curve used to link the
169 controlled suction ψ to the PEG solution concentration c was initially obtained by Williams
170 and Shaykewich (1969). It can be expressed as (Delage et al. 1998)

$$171 \quad \psi = 11c^2 \quad (2)$$

172 The suction ψ is in MPa and c is expressed in g PEG/ g water.

173 This equation indicates that the greater the solution concentration, the greater the imposed
174 suction. Semi permeable membranes are defined by their molecular weight cutoff (MWCO).

175 A membrane with a MWCO of 14 000 kg/mol has to be used with a PEG solution of 20 000
176 Da (Delage et al., 2008).

177 The main advantage of this technique compared with using oversaturated saline solutions is
178 that PEG solutions at controlled concentrations provide control of suction when the suction is
179 small. To ensure stable PEG concentration, a large bottle of PEG (1000 cm^3) was used, as
180 indicated in Figure 2 (b). The suctions applied by using the PEG solutions cross out to 0.1,

181 0.5, 1, and 2.8 MPa. These values were obtained by using solutions of PEG (20 000 Da) with
182 concentrations of 0.09, 0.21, 0.30, and 0.50 g PEG/g of water, respectively. Tests were also
183 performed by using pure water, which resulted in zero applied suction.

184 **3.4. Specimen installation and measurements**

185 Saturated salt solution techniques and the osmotic technique were adapted to control GCLs'
186 suction into oedometers cells. A series of four GCL specimens of comparable mass (Table 3)
187 were carefully placed into the oedometer cells, with special care taken not to lose bentonite
188 grains from the edge of the specimens. To speed up the vapour circulation process in the case
189 of saturated salt solution technique, that can take several weeks for high-density plastic clays,
190 vapour transfer through the specimen or along the boundaries of the specimen can be forced
191 by a venting circuit driven by an air pump (Yahia-Aissa, 1999; Blatz and Graham 2000). As
192 seen in Figure 2 (a), the closed-loop venting circuit consists of the following elements
193 connected in series: a porous stone at the base of the oedometer, a pneumatic pump, and a
194 bottle containing the oversaturated saline solution in a temperature-controlled bath.

195 In the case of osmotic technique method, the oedometric equipment (Figure 2 b) was used
196 according to Kassif and Ben Shalom (1971)'s set up and modified later by Delage et al.
197 (1992).

198 The PEG solutions were circulated over a closed circuit using a peristaltic pump which insures
199 the water transfer between the membrane and the GCL specimen.

200 The initial suction of GCLs was evaluated by measurements done on two comparable GCL
201 specimens by using a WP4 dew-point tensiometer (Decagon) that provided suction values of
202 135 MPa at water contents of 9.63%, respectively. Each of the four specimens was then
203 submitted to one of the four confining stresses: 10, 50, 100 and 200 kPa. These stresses were
204 applied prior to decreasing the suction along the wetting path from an initial suction of 135
205 MPa. The vapour circulation using salt solutions and liquid circulation using PEG solution

206 started when there was no change noticed on the GCL thickness. Two sets of four specimens
207 were used for both the oversaturated saline solution (four stresses were applied under imposed
208 suctions of 4.2 and 8.5 MPa) and the PEG solution (four stresses were applied under imposed
209 suctions of 0.1, 0.5, 1, and 2.8 MPa). The room temperature was maintained at 21 ± 0.5 °C.
210 The height of the specimen was monitored by a displacement gauge. Equilibrium was
211 evaluated when swell measurements reached 90% of the maximum swell (equilibrium criteria
212 for hydration provided by NF P84-705 as follows :

$$213 \quad \Delta h = \Delta h_{90} \frac{t}{t_{90} + t} \quad (3)$$

214 Δh_{90} corresponding to the maximum swelling at 90% of maximum swelling and t_{90} time
215 corresponding to 90 % of maximum swelling). We could thus determine time reaching
216 equilibrium by estimating the maximum swelling and establishing a criteria of equilibrium
217 which is reaching 90% maximum.

- 218 • Height measurements was always undertaken on the center of the specimen thanks to a
219 plate as for conventional oedometer,

220 Gravimetric water contents were determined at the end of each measurement (French standard
221 NF P 94-050).

222

223 **4. RESULTS AND DISCUSSION**

224 The GCL specimens were measured using both the SS and PEG procedures. Some standard
225 saturated oedometer measurements (OETs) were also conducted. The measurement program
226 is summarized in Table 3 and used suction between 0 and 8.5 MPa. For each measurement a
227 dry specimen was loaded into the oedometer and subjected to the desired stress prior to
228 imposing a suction less than the initial suction (135 MPa). The specimens were under
229 constant vertical stress during the measurements.

230

231 **4.1.Effect of confining stress on water-retention curve**

232 Figure 3 shows the suction as a function of gravimetric water content obtained with the SS,
233 PEG, and OET methods together with the point corresponding to the natural water content
234 with an initial suction of 135 MPa. The four points plotted for each applied suction (either by
235 SS or PEG) corresponds to the four different vertical loads applied. As is typically found, the
236 smaller the suction controlled, the higher the water content measured under the different
237 confining stresses between 10 and 200 kPa.

238 These results show that the influence of the applied stress is almost negligible for suctions
239 greater than 2.8 MPa. In this range of applied suction, the water content is comparable for the
240 four applied vertical loads. These results are consistent with those of Abuel Naga and
241 Bouazza (2010), who highlighted the insignificant effect of a 50 kPa confining stress on the
242 water retention of GCLs at suctions greater than 10 MPa, where swelling and water uptake
243 were less than at smaller suctions. This is the reason why only three normal stresses (<10
244 kPa, 100 kPa, and 200 kPa) were applied to specimens for suctions greater than 2.8 MPa.

245 At suctions less than 2.8 MPa, the effect of the confining stress on the GCL water content is
246 clearly apparent. At a given suction, more water is retained for a smaller confining stress.
247 Maximum water content occurs at zero stress (represented here in the semi-log graph of Fig. 4
248 at 0.1 kPa) with values ranging from 85% (less than 200 kPa confining stress) to 160% (less
249 than 10 kPa confining stress).

250 Figure 4 shows the change of the thickness of the oedometer specimens that occurred during
251 the measurements described in Figure 3. Figure 4 shows the change of the thickness volume
252 of the oedometer specimen as a function of time obtained under the four applied vertical
253 stresses (10, 50, 100, and 200 kPa) at controlled suction of 8.5, 4.2, 2.8, 1, 0.5, 0.1, and 0
254 MPa, respectively.

255 The initial response is a rapid compression observed when applying the load, which is typical
256 of unsaturated soils and corresponds to the rapid expulsion of air. All initial settlements
257 should be comparable. However, this is actually not the case because the initial mass differs
258 between the five different GCL specimens, as seen in Figure 5 and Table 3. Figure 5 shows
259 that a dispersion of about ± 0.5 in void ratio occurs for all stresses, a range comparable to that
260 obtained from the data of Beddoe et al. (2011) at a stress of 2 kPa. The data of Abuel Naga
261 and Bouazza (2010) also concur with this observation. Figure provides some information on
262 the compression properties of the dry GCL.

263 After the initial rapid settlement (which not exceed 2 hours), the GCL is subjected to
264 controlled suction from the saturated saline solution for the greater suctions or from the
265 controlled-concentration PEG solutions for lower suctions down to zero).

266 The increase of the settlement registered either when the suction decrease could be related to
267 some collapse mechanism. This latter represents an additional settlement of GCLs specimens'
268 occurring after the stabilization of the compression resulting from the application of the
269 confining stress. As have been explained by Tadeballi and Fredlund (1991), collapse
270 mechanism occurs with soils typically presenting an open type of structure with many void
271 spaces, which give rise to a metastable structure. It could be believed in this case that the
272 application of the confining stress and the decrease of the suction by controlled suction
273 techniques could lead to structural arrangement of grains bentonite's particules into GCLs
274 specimens. Collapse mechanism could be observed for example for 200 kPa of applied
275 confining stress. So Figure 4 shows that the change in GCL volume depends strongly on the
276 confining stress the applied suction, and the grain size distribution of the bentonite as part of
277 the GCL.

278 Under the highest suction of 8.5 MPa and after the initial compression process, the GCL and
279 the GCL volume does not significantly change, which shows that the decrease in suction from

280 the initial value of 135 MPa down to 8.5 MPa does not significantly affect the overall volume
281 in spite of some water being absorbed by the specimen. This means that hydration occurs
282 within the bentonite grains with little volume change of the grains themselves.

283 Volume changes induced by suction decrease under constant stress and are more apparent
284 under suctions less than 1 MPa (Figure 6). As could be seen in Figure 6, change in thickness
285 is very close for each confining stresses for suction higher than 1 MPa.

286 Under this suction, the changes in volume are typical of unsaturated swelling soils.
287 Specifically, the results show:

- 288 - (i) no swelling at the largest stress (200 kPa), which corresponds to the collapse
289 mechanism,
- 290 - (ii) no significant swelling at 100 kPa stress,
- 291 - (iii) swelling at the two smaller stresses (10 and 50 kPa).

292 Under the suction of 0.5 MPa, the final settlement under a 200 kPa compressive stress is -2
293 mm (comparable to that at a suction of 1 MPa), whereas some settlement due to suction
294 increase is observed for a compressive stress of 100 kPa. As expected, the swelling observed
295 for smaller stresses (10 and 50 kPa) is greater under a suction of 0.5 MPa compared with that
296 obtained previously under a larger suction of 1 MPa.

297 Greater swelling is observed when the specimen is under 0.1 MPa suction. Settlement still
298 occurs under 100 and 200 kPa of compressive stress (the constant value observed at stresses
299 below 100 kPa is due to a technical problem related to a blocked oedometer piston). For
300 compressive stresses less than 200 kPa, the settlement changes less (<2 mm) than at 0.5 MPa
301 of suction and 200 kPa of compressive stress.

302 Finally, for the GCL specimen under zero suction (obtained by circulating pure water in the
303 osmotic oedometer), the results agree well with previous measurements: no swelling occurs

304 under a compressive stress of 200 kPa, whereas all other GCL specimens swell when
305 subjected to lower stresses (100, 50, and 10 kPa).

306 The decrease in porosity and change in the pore structure of the bentonite layer under greater
307 compressive stress is expected to result in a reduction of the GCL's saturated conductivity. To
308 investigate this aspect, constant-head saturated permeability measurements were done on
309 GCL specimens provided from the same GCL sample in an oedopermeameter (230 mm in
310 diameter and 9 mm in height) under a 10 cm hydraulic head, using the protocol of the French
311 standard NF P84-705. Once the specimens were saturated, the constant flow rate traversing
312 the specimens was measured, providing the saturated hydraulic conductivity via Darcy's law.
313 The results show that the hydraulic conductivity of a saturated GCL decreased by 59% from
314 3.10×10^{-11} to 1.85×10^{-11} m/s when the confining stress was increased from 10 to 200 kPa.

315 **4.2.Comparison with published data**

316 Figure 7 shows the gravimetric water content as a function of suction under 10 kPa
317 compressive stress obtained in the present study. These data are compared with similar data
318 obtained under free-swell conditions in other studies of GCLs (Barroso et al., 2006b; Daniel
319 et al., 1993; Hanson et al., 2013) and in studies of compacted bentonites for research into
320 radioactive-waste disposal (Yahia-Aissa et al., 2001; Villar and Lloret, 2004; Delage et al.,
321 2006). Note that, due to compaction, bentonite used for radioactive-waste disposal is
322 significantly denser than the granular bentonite contained in GCLs. The suction applied to the
323 compacted bentonite is therefore generally higher.

324 The data shown in Figure 7 indicate a relatively good agreement between the results obtained
325 in the present study with GCLs and published results from studies of either GCLs or
326 compacted bentonites. The only exception is for FoCa7 clay (Yahia-Aissa et al., 2001), but
327 the difference here is attributed to the material not being a pure smectite and having a
328 significant calcium content. This agreement confirms that WRCs are independent of the as

329 received density of bentonites, which is attributed to water adsorption occurring within the
330 bentonite grains. This means that water absorption is mainly governed by local water-clay
331 physicochemical interactions within the bentonite grains.

332 Figure 8 compares the data of this work with published WRCs determined from GCLs under
333 confining stress (Abuel Naga and Bouazza, 2010; Beddoe et al., 2011). Not surprisingly,
334 WRCs obtained from GCLs under confining stress agree better with our results, illustrating
335 clearly the significant influence of confining stress on the water-retention properties of GCLs.

336 The results of the present study agree reasonably well with the data obtained by Abuel-Naga
337 and Bouazza (2010) from GCLs under 50 kPa of confining stress. The agreement with the
338 data of Beddoe et al. (2011), obtained from a GCL under a small confining stress of 2 kPa, is
339 less satisfactory: they observed higher water content at high suction (above 20 MPa) and
340 lower water content at low suction (below 0.1 MPa). Note that significant differences existed
341 between GCLs 1, 2, 3 and 4 tested by Beddoe et al (2011). In addition, compared with the
342 granular bentonite used in the GCLs for present study, the bentonite powder in the GCLs used
343 by Beddoe et al. (2011) is more strongly confined because of a thermal treatment and the
344 scrim reinforcement, which results in a much more strongly bonded structure compared with
345 the needle-punched structure of the GCL used in this study. These data tend to show an effect
346 of the GCL structure on its water retention behaviour: a stronger structure could lead to a
347 significant decrease in water uptake and reduced swelling of the bentonite.

348

349 **4.3. Equations for water retention as a function of stress**

350 A quantitative equation for water retention in a GCL under various stresses is derived based
351 on two well-known equations for WRCs: namely, that of van Genuchten (1985) and of
352 Fredlund and Xing (1994). The van Genuchten equations is

353
$$\theta(\psi, T_0) = \theta_r + \frac{\theta_s - \theta_r}{(1 + |\alpha\psi|^n)^m}, \quad \theta_r \leq \theta \leq \theta_s, \quad (4)$$

354 where θ is the volumetric water content (m^3/m^3), T_0 is the temperature $= 21 \pm 0.5$ °C, θ_r is the
 355 residual water content (m^3/m^3) at high suction, θ_s is the water content (m^3/m^3) at zero suction,
 356 ψ the suction (m), and α (1/m), n , and m are fitting parameters (with $m = 1 - 1/n$).

357 In clayey soils, θ_r is often assumed to be equal to zero (Babu et al., 2002). In this case, Eq. (4)
 358 simplifies to

359
$$\theta(\psi, T_0) = \theta_s \left(\frac{1}{(1 + |\alpha\psi|^n)} \right)^m. \quad (5)$$

360 The Fredlund and Xing equation is

361
$$\theta = \theta_s \left[1 - \frac{\ln\left(1 + \frac{\psi}{\psi_r}\right)}{\ln\left(1 + \frac{10^6}{\psi_r}\right)} \right] \left[\frac{1}{\ln\left[e + \left(\frac{\psi}{a_f}\right)^{n_f}\right]} \right]^{m_f}, \quad (6)$$

362 where θ is the volumetric water content (m^3/m^3), θ_s is the water content (m^3/m^3) at zero
 363 suction, ψ is the suction (kPa), ψ_r is the residual suction (kPa), and a_f (kPa), n_f , and m_f are
 364 fitting parameters.

365 Given the comparable shapes of the WRCs obtained under the four different stresses (10, 50,
 366 100, 200 kPa), a single set of parameters (excluding θ_s , which depends on the confining
 367 stress) was obtained from the van Genuchten and the Fredlund and Xing equations for all four
 368 WRCs. For these fits, the WRCs were normalized to their water content at zero suction θ_s .
 369 The single set of parameters obtained from both equations is presented in Table 5, together
 370 with the values of water content at zero suction θ_s (which remains the only parameter
 371 dependent on stress in both equations). The following formulas for θ_s as a function of stress
 372 were obtained:

373 - van Genuchten fit: $\theta_s = 0.9507e^{-0.003\sigma}$ (with $R^2 = 0.9665$), (7)

374 - Fredlund and Xing fit: $\theta_s = 0.959e^{-0.003\sigma}$ (with $R^2 = 0.9771$) (8)

375

376 The corresponding fits are shown in Figure 9. Both the van Genuchten and Fredlund and Xing
377 formulas fit reasonably well to the four experimental WRCs, although they slightly
378 underestimate the volumetric water content at the highest stress of 200 kPa.

379 To account for the dependence on stress of the two WRC equations [Eqs. (5) and (7)] adopted
380 here, two more parameters are necessary. These parameters come from the equations for
381 water content as a function of stress at zero suction θ_s , which are expressed in Eqs. 7 and 8.

382

383 The volumetric water content θ as a function of suction ψ and applied stress σ are represented
384 in three-dimensional graphs in Figs. 10(a) and 10(b) for Eqs. (5) and (6), respectively. These
385 representations are comparable to state surfaces that, along a wetting path, govern the changes
386 in volume and degree of saturation of unsaturated soils (Matyas and Radhakrisna 1968).

387 Each surface plotted in Figure 9 clearly shows the dependence of the volumetric water content
388 on the applied vertical stress as suction decreases. When the vertical stress increases from 0 to
389 300 kPa, the water content increases from 0.39 to 0.92 at zero suction whereas it increases
390 from 0.09 to 0.28 at a 5 MPa suction. This kind of representation makes it possible to predict
391 the volumetric water content and other state parameters of unsaturated GCLs under specific
392 site conditions.

393

394 5. CONCLUSION

395 The dependence on stress of the water-retention of a needle-punched GCL was investigated
396 by controlled suction oedometer measurements under constant confining stress. The suction
397 was varied to determine the wetting path. To circumvent the capillary barrier effect of the

398 carrier geotextile, the vapour-control technique was used. To obtain the two largest suctions
399 (4.2 and 8.5 MPa), the standard technique of controlling relative humidity by using a saturated
400 saline solution was used. For smaller suctions (0.1, 0.5, 1 and 2.8 MPa), the osmotic
401 technique was adapted to control vapour by using calibrated concentrations of PEG solutions,
402 ensuring a more continuous series of applied suctions along the wetting path, down to zero
403 suction.

404 The experimental water-retention curves obtained under various confining stress allowed the
405 following conclusions to be drawn:

- 406 • Increasing vertical stress resulted in a decrease in water uptake along the wetting
407 path accompanied by a reduction in the swelling capacity and in the saturated
408 hydraulic conductivity of the GCL.
- 409 • The WRCs obtained under the smallest stress (10 kPa) agree fairly well with
410 existing WRCs of either GCLs or compacted bentonites used in radioactive-waste
411 disposal. This results indicates that water retention in bentonites depend only
412 slightly on their density, which is attributed to the predominance of
413 physicochemical clay-water interactions.
- 414 • The WRCs obtained with the GCLs under stress also agreed with previously
415 published WRCs for GCLs under stress.
- 416 • Examination of published data also reveals the significant effect of GCL structure
417 on its ability to retain water.
- 418 • Two well-known formulas for WRCs (van Genuchten, 1985 and Fredlund and
419 Xing, 1994) correctly fit the data obtained in this study. By fitting these equations
420 to normalized water-retention curves, two new equations that include stress effects
421 are proposed for WRCs. The corresponding surfaces are represented in three-

422 dimensional graphs that show the dependence of water content on stress and
423 suction along a wetting path.

424 • The possible validity of the state-surface concept applied to GCLs under stress was
425 discussed. The validity of this concept would likely be confirmed by constant-
426 suction compression measurements on hydrated bentonites.

427 • Three-dimensional graphs that show the effects of stress on water retention in
428 GCLs appear to be a useful way to illustrate the observed trends; namely, that
429 water uptake is reduced in GCLs under larger stress.

430

431 The two new equations for volumetric water content of a GCL as a function of both suction
432 and stress will certainly help hydromechanical numerical modeling of GCL hydration under
433 specific site conditions, where GCLs are submitted to water infiltration under the weight of
434 the supported waste layers. From a practical point of view, this study also emphasize on the
435 recommendation of rapidly covering GCLs once they are installed so as to make them more
436 rapidly operational and hydrated in barrier systems. In addition, immediately after GCL
437 installation in geotechnical applications, a solid bonding structure is also recommended to
438 naturally confine the GCL, even under low stress.

439

440 **6. ACKNOWLEDGMENTS**

441 The authors gratefully acknowledge CETCO for providing the geosynthetic clay liners used in
442 this study and the Navier/CERMES team and M. E. De Laure (Ecole des Ponts/ParisTech) for
443 providing the osmotic oedometers. Finally, IRSTEA Antony (France) is also acknowledged
444 for providing funding for a good portion of this work.

445

446 **7. REFERENCES**

447 Abuel-Naga, H.M., Bouazza, A., 2010. A novel laboratory technique to determine the water
448 retention curve of geosynthetic clay liners. *Geosynthetics International*. 17(5), 313–322.

449 Abuel-Naga, H.M., Bouazza, A., 2011. Effects of temperature and thermal gradient on
450 thermocouple psychrometer measurements. *Géotechnique*. (61) 10, 875–88

451 AFNOR 2008. NF P 84-705. Geosynthetic barriers — Determination of the swelling, flow
452 and permeability characteristics of geosynthetic clay liners (GCL) using an
453 oedopermeameter — Characterisation test and performance test.

454 Azad, F.M., Rowe, R.K., El-Zein, A., Airey, D.W., 2011. Laboratory investigation of
455 thermally induced desiccation of GCLs in double composite liner systems. *Geotextiles and*
456 *Geomembranes* 29 (6), 534–543.

457 Babu, G.L.S., Sporer, H., Gartung, E., 2002. Desiccation behavior of selected geosynthetic
458 clay liner. *Proceedings of the international symposium IS Nuremberg 2002*. Nuremberg,
459 Germany, 295–302.

460 Barroso, M., Touze-Foltz, N., Saidi, F., 2006b. Validation of the use of filter paper suction
461 measurements for the determination of GCLs water retention curves. *Proceedings 8ICG,*
462 *Geosynthetics, Yokohama, Japan*, 171–174.

463 Beddoe, R. A., Take, W. A., Rowe, R. K., 2010. Development of suction measurement
464 techniques to quantify the water retention behaviour of GCLs. *Geosynthetics International*.
465 17(5), 301–312.

466 Beddoe, R. A., Take, W. A., Rowe, R. K., 2011 Water-Retention Behavior of Geosynthetic
467 Clay Liners.” *Journal of geotechnical and geoenvironmental engineering*. Novembre 2011,
468 1028–1038.

469 Blatz, J.A., Graham, J., 2000. A method for controlled suctions in triaxial testing.
470 *Géotechnique*. 50(4), 465–470.

471 Bouazza, A., 2002. Geosynthetic clay liners. *Geotextiles and Geomembranes*. 20(1),. 1–17.

472 Daniel, D.E., Shan, H-Y., Anderson, J.D., 1993. Effects of Partial Wetting on the
473 Performance of the Bentonite Component of a Geosynthetic Clay Liner. Proceedings of
474 Geosynthetics'93. Vol. 3. IFAI. St. Paul. USA, 1482–1496.

475 Delage, P., Cui, Y.J., 2008. An evaluation of the osmotic method of controlling suction.
476 Journal of Geomechanics and Geoengineering. 3 (1), 1–11.

477 Delage, P., Cui, Y.J., Yahia–Aissa, M., De Laure, E., 1998. On the unsaturated hydraulic
478 conductivity of a dense compacted bentonite. Proceedings of the 2nd International
479 Conference on Unsaturated Soils. UNSAT'98. Beijing. 1, 344–349.

480 Delage, P., Howat, M., Cui, Y.J., 1998. The relationship between suction and swelling
481 properties in a heavily compacted unsaturated clay. Engineering Geology. 50 (1-2), 31–48.

482 Delage, P., Marcial, D., Cui, Y. J., Ruiz, X., 2006. Ageing effects in a compacted bentonite: a
483 microstructure approach. Géotechnique. 56(5), 291–304.

484 Delage, P., Romero, E., Tarantino, A., 2008 Recent developments in the techniques of
485 controlling and measuring suction in unsaturated soils. Keynote Lecture. Proc. 1st Eur.
486 Conf. on Unsaturated Soils. Durham, 33–52.

487 Delage, P., Suraj De Silva, G.P.R., Vicol, T., 1992. Suction controlled testing of non-saturated
488 soils with an osmotic consolidometer. 7th Int. Conf. Expansive Soils. Dallas, 206–211.

489 EN 14196, 2003. Geosynthetics. Test Methods for Measuring Mass per Unit Area of Clay
490 Geosynthetic Barriers. European Committee for Standardization, Brussels, Belgium.

491 EN ISO 9863-1, 2005. Geosynthetics – Determination of Thickness at Specified Pressures –
492 Part 1: Single Layers. European Committee for Standardization, Brussels, Belgium.

493 Fredlund, D.G, Xing. A., 1994. Equations for the soil–water characteristic curve. Canadian
494 Geotechnical Journal. 31, 533–546.

495 Hanson, J.L., Risken, J.L., Yesiller, N., 2013. Moisture-Suction relationship for geosynthetic
496 clay liners. Proceedings of the 18th conference on soil mechanics and geotechnical
497 engineering. Paris. France, 3025–3028.

498 Kassif, G., Ben Shalom., A., 1971. Experimental relationship between swell pressure and
499 suction. Géotechnique. 21, 245–255.

500 Lloret, A., Villar, M.V., Sánchez, M., Gens, A., Pintado, X., Alonso. E.E., 2003. Mechanical
501 behavior of heavily compacted bentonite under high suction changes. Géotechnique. 53 (1),
502 27–40.

503 Matyas, E.L., Radhakrishna, H.S. 1968. Volume change characteristics of partially saturated
504 soil. Géotechnique, 18, 432–448

505 Siemens, G., Take, W. A., Rowe, R., K., Brachman, W. I., 2011. Numerical investigation of
506 transient hydration of unsaturated geosynthetic clay lines.geosynthetic international. 19(3),
507 232–251.

508 Siemens, G., Take. W.A., Rowe, R. K., Brachman, R., 2013. Effect of confining stress on the
509 transient hydration of unsaturated GCLs. Proceedings of the 18th conference on soil
510 mechanics and geotechnical engineering. Paris. France, 1187–1190

511 Southen, J.M., Rowe, R.K., 2004. Investigation of the Behavior of Geosynthetic Clay Liners
512 Subjected to Thermal Gradients in Basal Liner Applications. Journal of ASTM
513 International. 1(2).

514 Southen, J.M., Rowe., R. K., 2007. Evaluation of the water retention curve for geosynthetic
515 clay liners. Geotextiles Geomembranes. 25(1), 2–9.

516 Tadepalli, R., Fredlund, D.G., 1991. The collapse behavior of a compacted soil during
517 inundation. Can. Geotech. J. 28, 477–488.

518 van Genuchten, M. T. H., 1985. A closed-form *equation* for predicting the hydraulic
519 conductivity of unsaturated soils.”Soil Sci. Soc. Am. J. 44(5), 892–898.

520 Villar, M.V., Lloret, A., 2004. Influence of temperature on the hydro-mechanical behaviour of
521 a compacted bentonite. *Applied Clay Science*. 26, 337–350.

522 Villar, M.V., Lloret, A., Romero, E., 2003. Thermo-mechanical and geochemical effects on
523 the permeability of high-density clays. In: *Proceedings of the International Workshop Large*
524 *Scale Field Tests in Granite. Advances in Understanding and Research Needs*. Universitat
525 *Polite`cnica de Catalunya-ENRESA*. Sitges. November 12–14.

526 Williams, J., Shaykewich, J., 1969. An evaluation of polyethylene glycol (PEG) 6000 and
527 PEG 20 000 in osmotic control of soil water matric potential. *Canadian Journal of Soil*
528 *Science*. 35, 206–221.

529 Yahia-Aissa, M., 1999. Comportement hydromécanique d'une argile gonflante fortement
530 compactée. Thèse de doctorat. Ecole nationale des ponts et chaussées. Cermes. Paris. 241 p.

531 Yahia-Aissa, M., Delage, P., Cui, Y.J., 2001. Suction-water relationship in swelling clays.
532 *Clay science for engineering*. IS-Shizuoka International Symposium on Suction. Swelling.
533 *Permeability and Structure of Clays*. Adachi & Fukue eds. Balkema. 65–68.

534 Zornberg, J. G., Bouazza, A., Mc Cartney, J.S., 2010. Geosynthetic capillary barriers: Current
535 state of knowledge. *Geosynthetics International*. 17(5), 273–300.

536

537 Table 1. Published investigations of GCL water-retention curves.

Authors	Used technique	Confining stress (kPa)	Water cycle
Daniel et al. (1993)	Thermocouple Psychrometer (SCM) and vapour equilibrium (MCM)	0	Wetting path
Southen and Rowe (2004)	Pressure plate technique (SCM)	0	Drying
Barroso et al. (2006b)	Filter Paper (MCM)	0	Wetting path
Southen and Rowe (2007)	Pressure plate (SCM) and pressure membrane extractors (SCM)	0-0.5-3-100	Drying path
Abuel Naga and Bouazza (2010)	Thermocouple psychrometer (MCM) and a Capacitive relative humidity sensor (MCM)r	50	Wetting path
Beddoe et al. (2010)	High-capacity tensiometers (MCM) and capacitive relative humidity sensors (MCM)	2	Drying path
Beddoe et al. (2011)	High-capacity tensiometers (MCM) and capacitive relative humidity sensors (MCM)	2	Wetting/Drying path
Henson et al. (2013)	Pressure plate-Filter paper and relative humidity methods	0	Wetting/Drying path

538 “SCM” stands for “suction-control method” and “MCM” stands for “moisture-control method.”

539

540 Table 2 main features of the GCL studies

Materials	Properties	values
GCL	Thickness under 10 kPa EN ISO 9863-1 [m]	8×10^{-3}
	Mass per unit area EN 14196 [kg/m ²]	6.1
	Hydraulic conductivity NF P 84 705 under 10-160 kPa [m/s]	$3.10 \times 10^{-11} - 1.95 \times 10^{-11}$
	Bonding process	Needle punched
Cover geotextile	Type	Woven
	Mass per unit area EN 14196 [kg/m ²]	0.1
Benonite	Type	Granular sodium
	Mass per unit area EN 14196 [kg/m ²]	5.80
	Natural water content [%]	9.63
Carrier geotextile	Type	Non woven
	Mass per unit area EN 14196 [kg/m ²]	0.2

541

542 Table 3 Summary of measurements made to determine WRCs of GCLs.

Specimen	Method used	Controlled suction [MPa] [MPa]	Confining stress [kPa] [kPa]	Initial mass of GCL specimen [g] specimens
1	SS	8.5	10	23.09
2	SS	8.5	50	22.62
3	SS	8.5	200	22.29
4	SS	4.2	10	23.59
5	SS	4.2	10	23.64
6	SS	4.2	50	21.54
7	SS	4.2	200	25.3
8	PEG	2.8	10	24.57
9	PEG	2.8	50	23.02
10	PEG	2.8	200	22.54
11	PEG	1	10	23.82
12	PEG	1	50	23.94
13	PEG	1	50	24.51
14	PEG	1	100	22.65
15	PEG	1	200	23.97
16	PEG	0.5	10	22.99
17	PEG	0.5	10	23.89
18	PEG	0.5	50	22.52
19	PEG	0.5	100	22.41
20	PEG	0.5	200	23.34
21	PEG	0.1	10	24.52
22	PEG	0.1	50	23.09

23	PEG	0.1	100	24.47
24	PEG	0.1	200	22.70
25	PEG	0	10	24.12
26	OET	0	10	23.55
27	OET	0	50	24.68
28	PEG	0	50	23.05
29	OET	0	100	24.69
30	PEG	0	100	22.46
31	OET	0	200	22.99
32	PEG	0	200	21.43

543 “SS” stands for the vapour-equilibrium technique by oversaturated saline solution. “OT” stands for “osmotic technique” and

544 “OET” stands for “oedometric technique.”

545

546 Table 4 Properties of salts used in this work (adapted from Delage et al., 1998).

Saturated salt solutions	Relative Humidity controlled [%]	Suction [MPa]	Solubility [g/l]	Molar mass [g mol ⁻¹]
K ₂ SO ₄	97	4.2	111	174.26
KNO ₃	94	8.5	320	174.25

547

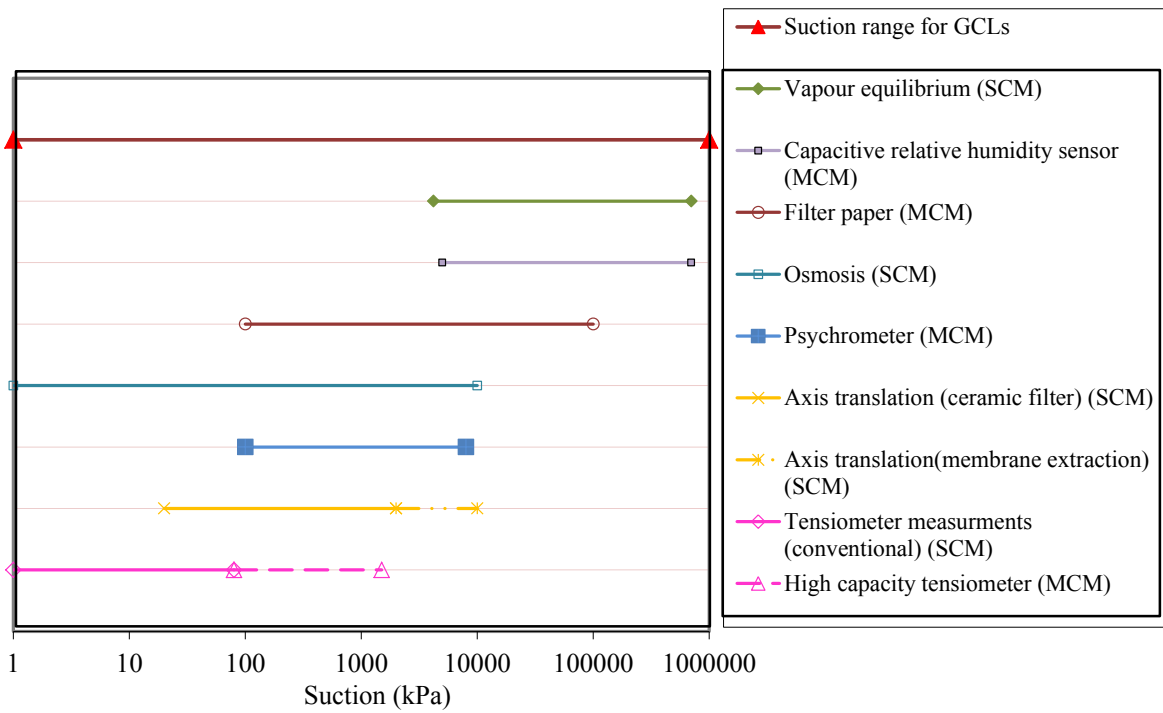
548

549 Table 5 Values of parameters obtained by fitting WRCs from Fig. 8 to Eqs. (4) and (5). Prior to fitting, WRCs
 550 were normalized to their water content at zero suction.

Model		Van Genuchten (1980)		Fredlund and Xing (1994)			
Fitting parameter	$\theta_s (\text{m}^3/\text{m}^3)$	α (1/m)	n	a_f (kPa)	n_f	m_f	ψ_f (kPa)
10 kPa	0.97	0.16	1.35	100	0.73	1.10	3326
50 kPa	0.79						
100 kPa	0.71						
200 kPa	0.54						

551

552



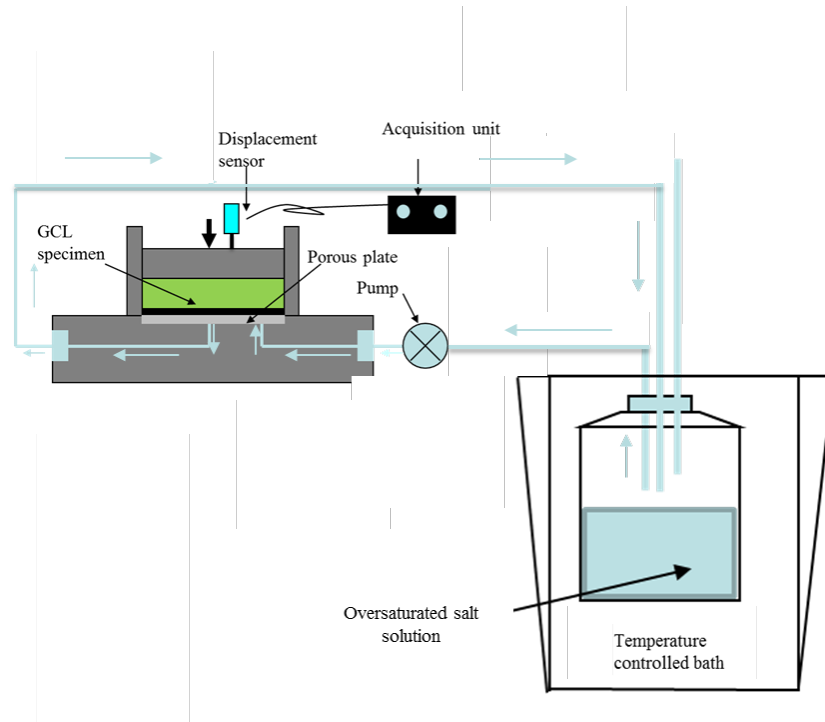
554

555 SCM: suction control method; MCM: moisture control method

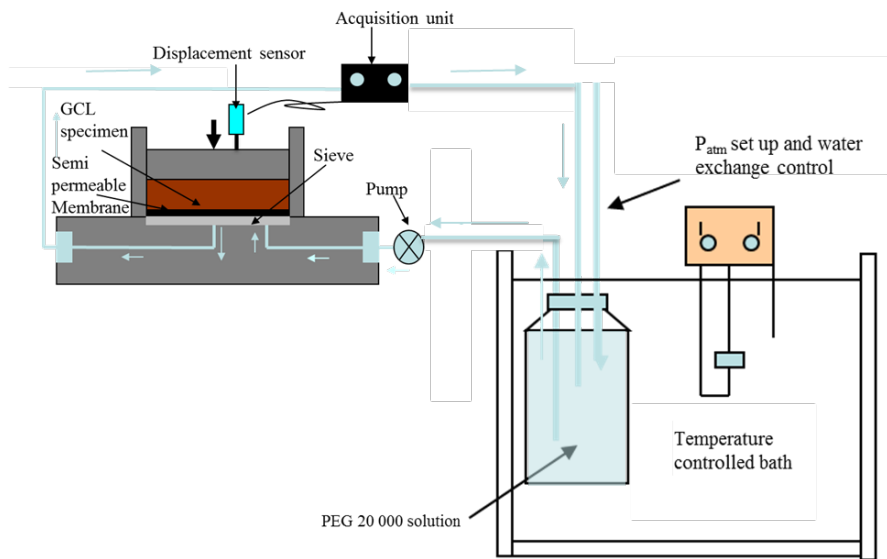
556 Figure 1. Applicable ranges for techniques to control or measure suction (modified from Likos and Lu 2003).

557

558



(a)



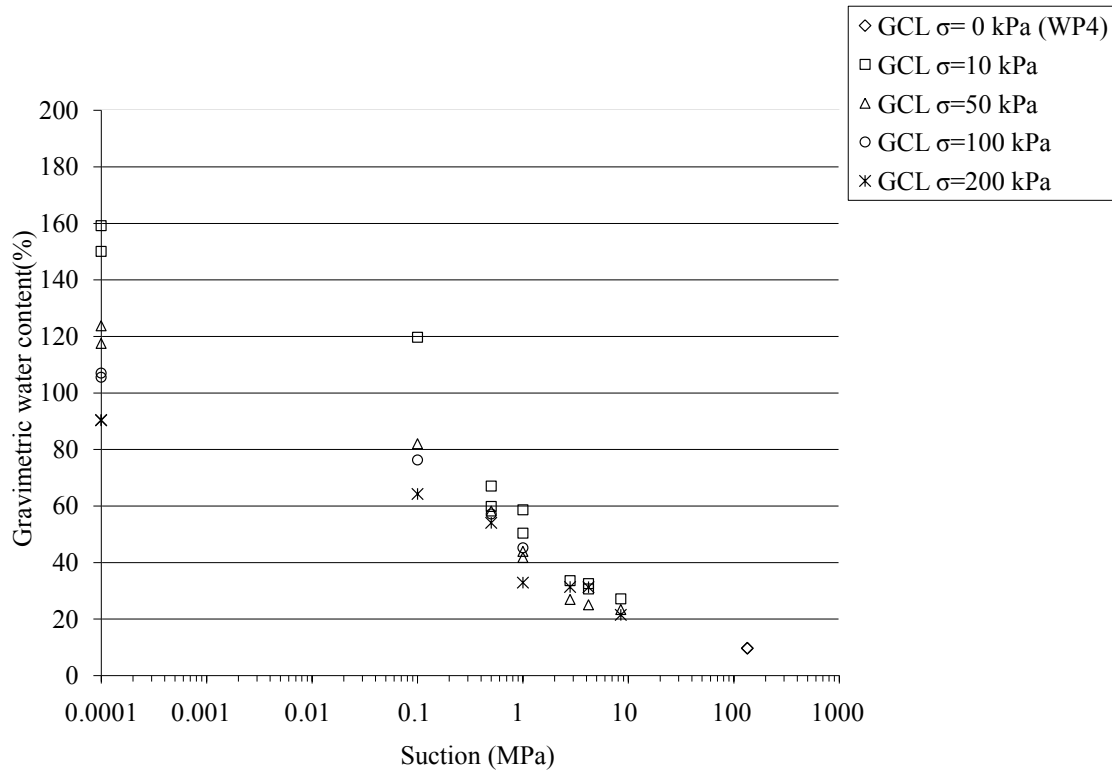
(b)

Figure 2. Representations of methods used to control GCLs specimens' suction on oedometric cells (a) saturated salt solution by circulated vapour. (b) Osmotic technique with circulated PEG solutions (adapted from Delage and Cui, 2008).

569

570

571



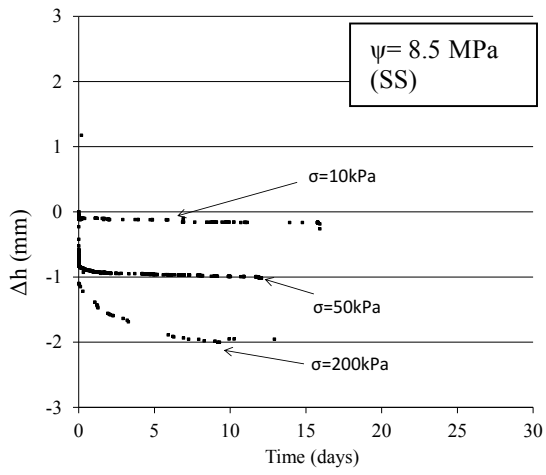
573

574

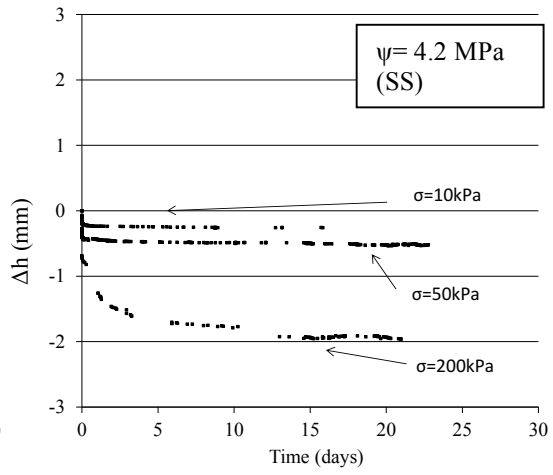
Figure 3. Water retention along the wetting path under vertical stresses of 10, 50, 100, and 200 kPa.

575

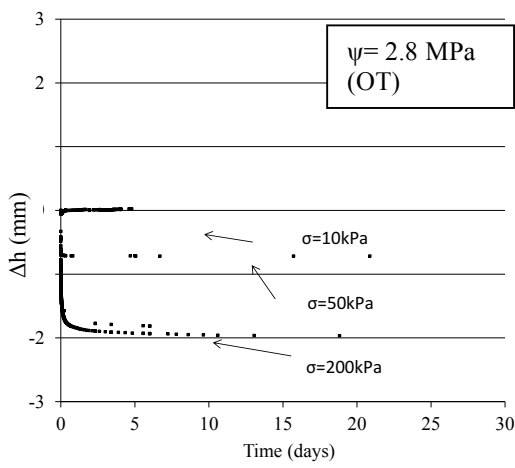
576



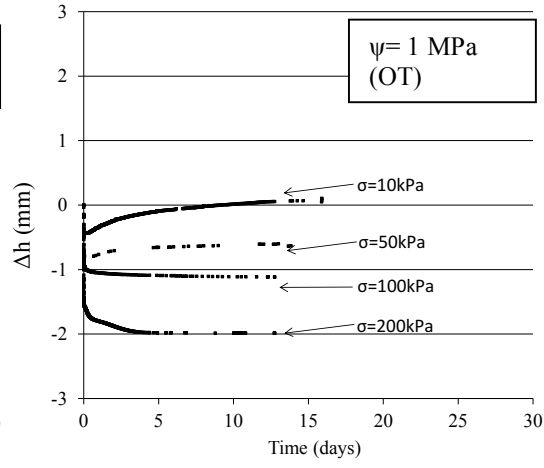
(a)



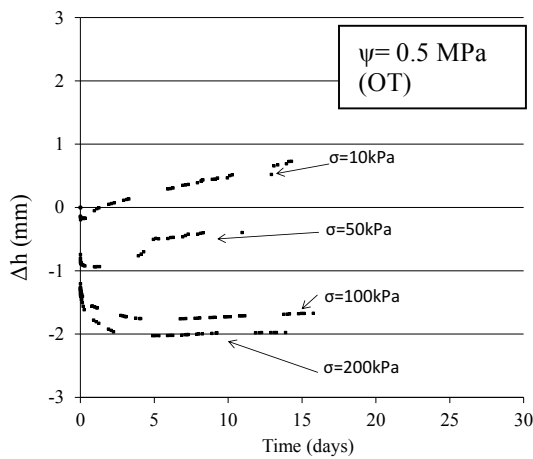
(b)



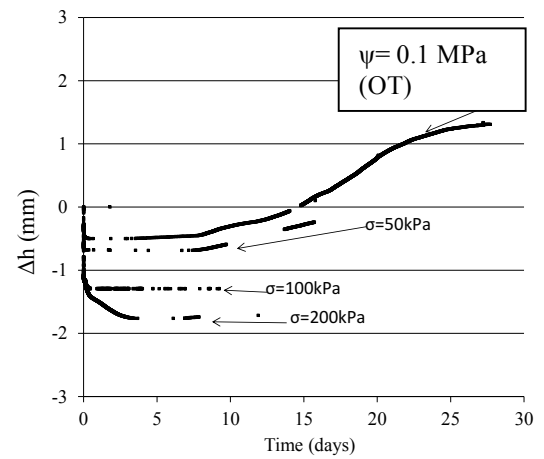
(c)



(d)



(e)



(f)

577

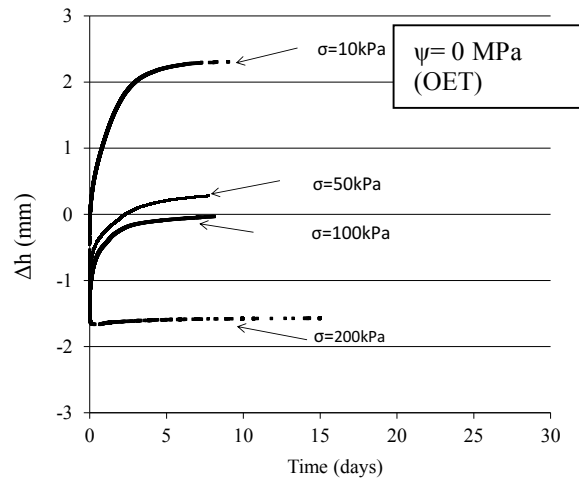
578

579

580

581

582



583

584

(g)

585 Figure 4. Change in Thickness of GCL specimens as a function of time for different confining stresses σ and for

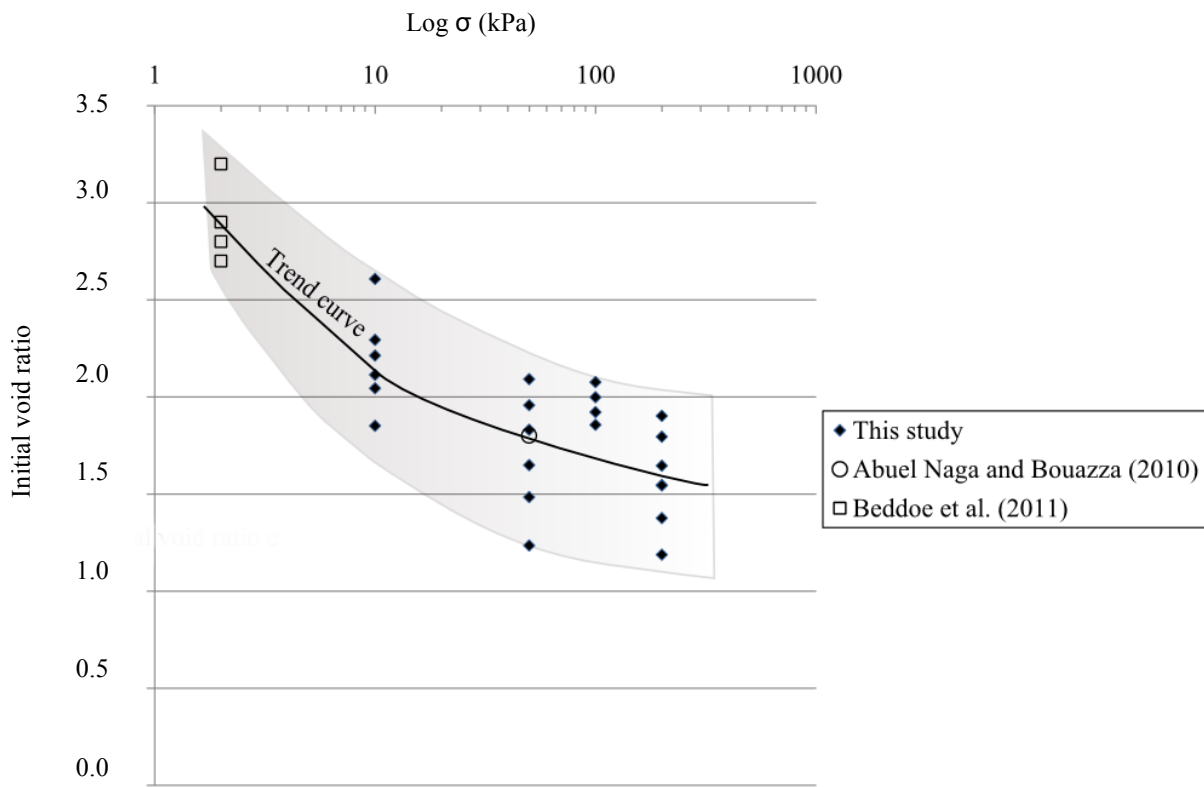
586

final suctions reached starting from initial suction of 135 MPa.

587

588

589



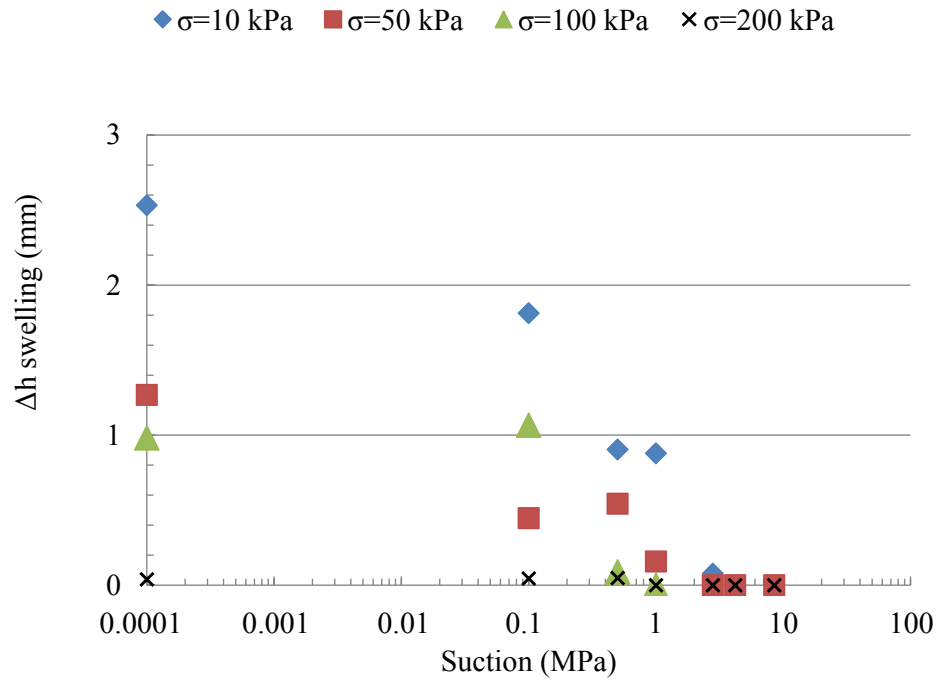
590

591 Figure 5. Initial void ratio as a function of the logarithm of the stress for dry GCLs (data from all measurements)

592

compared to published data.

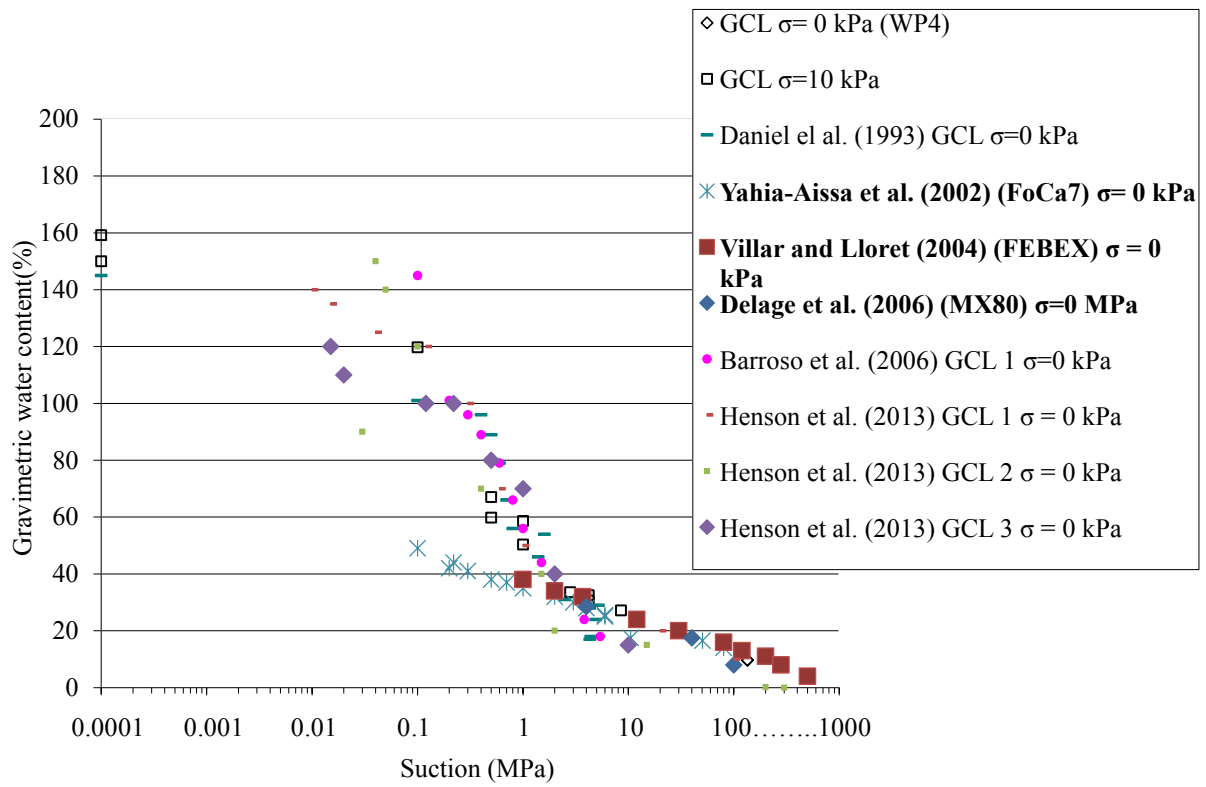
593



594

595 Figure 6 Comparison of changing height between GCLs specimens with suction as a function of confining stress

596

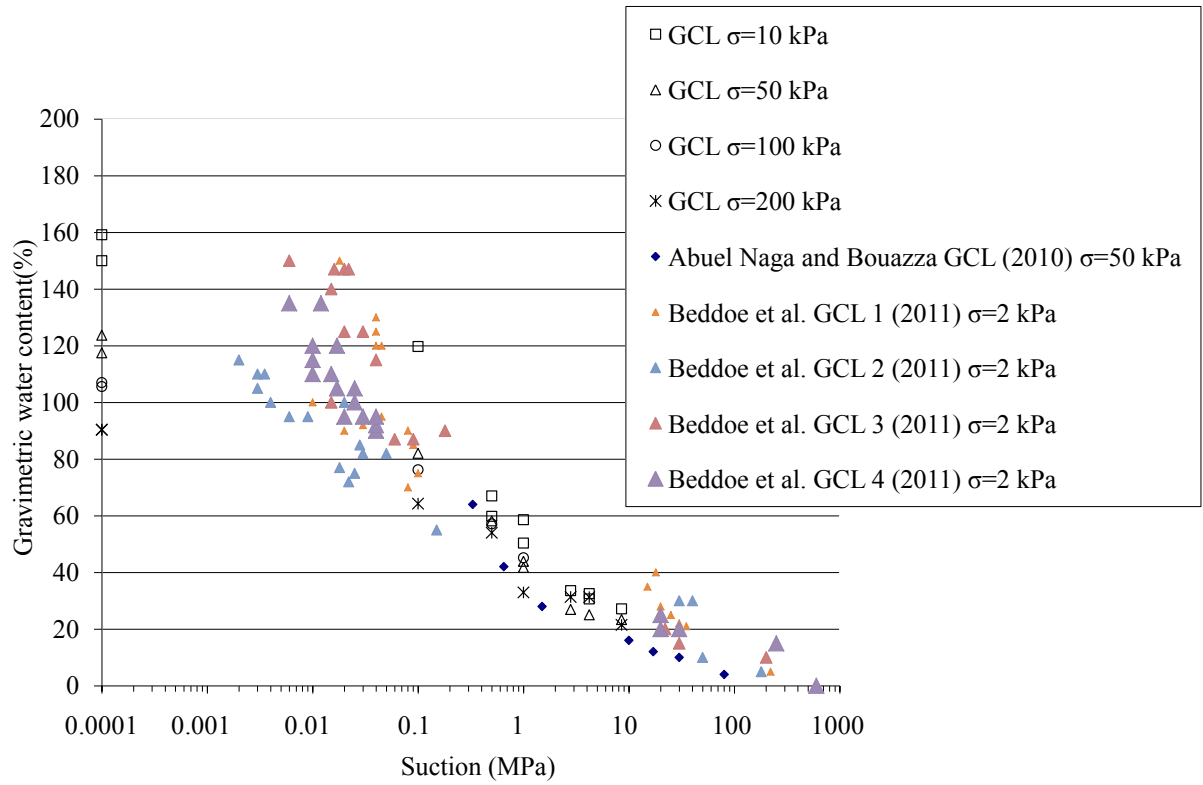


598

599 Figure 7. Comparison of wetting path water-retention data obtained in present study with published results for

600 GCLs and bentonites (deeply-buried). All data were acquired under free-swell conditions.

601



602

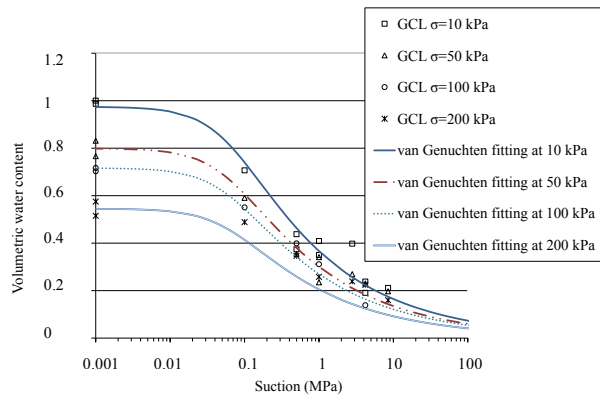
603

604

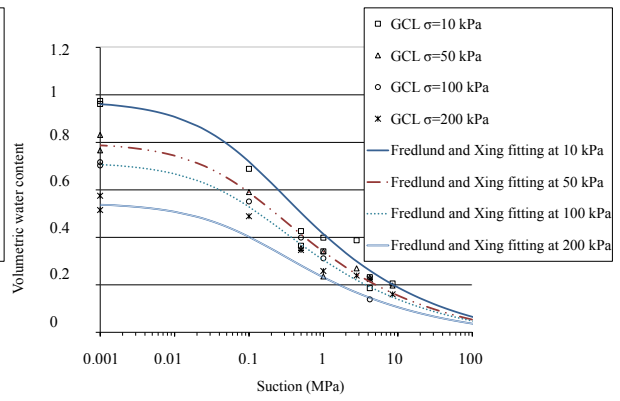
605

606

Figure 8 Wetting path water-retention data obtained in the present study compared with published results. All data were acquired with GCLs under nonzero confining stress.



(a)



(b)

Figure 9. Fits to experimentally determined WRCs at various vertical stresses using (a) van Genuchten's equation (4) and (b) Fredlund and Xing's equation (5).

607
608

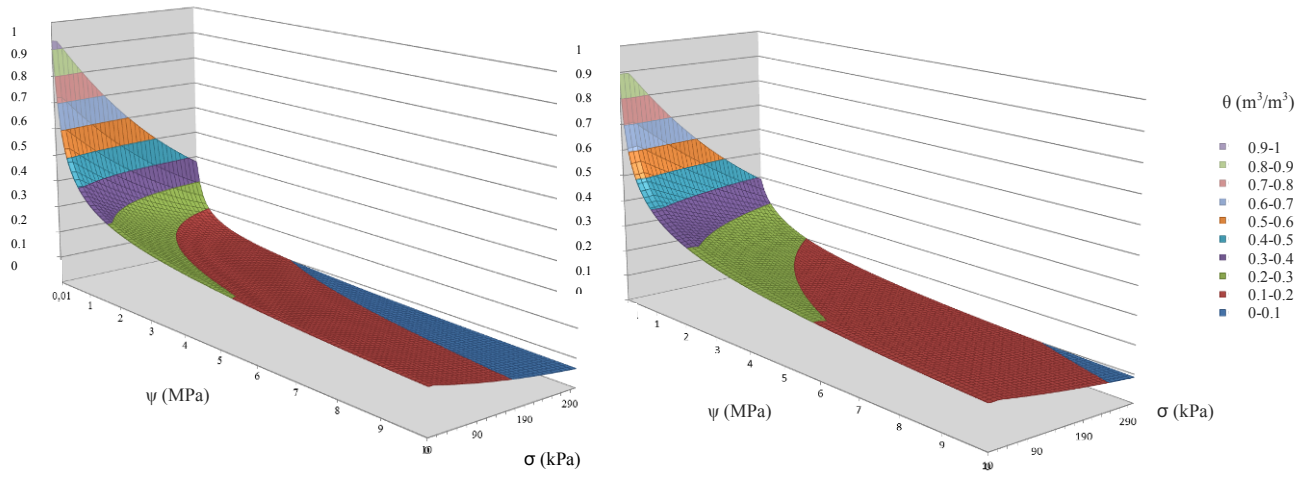
609

610

611

61 θ (m³/m³)

θ (m³/m³)



613

614

615 Figure 10 Dependence of WRCs on stress σ for GCL [$\theta = f(\psi, \sigma)$] based on (a) van Genuchten equation (4) and

616

(b) on Fredlund and Xing equation (5).